

Metamagnetism of a noncollinear antiferromagnet: the Jahn-Teller garnet $\text{Ca}_3\text{Mn}_2\text{Ge}_3\text{O}_{12}$

Z. A. Kazei, N. P. Kolmakova, D. I. Sirota, and V. I. Sokolova
M. V. Lomonosov State University, Moscow

(Submitted 1 February 1983)

Pis'ma Zh. Eksp. Teor. Fiz. **37**, No. 5, 240–243 (5 March 1983)

The metamagnetic phase transition in the crystal $\text{Ca}_3\text{Mn}_2\text{Ge}_3\text{O}_{12}$, induced by an external magnetic field, is investigated with the help of magnetostriction measurements at 4.2 K. The unusual phase diagrams in the (001) and (010) planes, obtained in the experiment, are described by a model of an anisotropic metamagnet with four local anisotropy axes.

PACS numbers: 75.30.Kz, 75.80. + q, 75.50.Ee

One of the manifestations of the cooperative Jahn-Teller effect in compounds with the garnet structure¹ is the noncollinear, eight-sublattice antiferromagnetic (AF) structure, which, according to neutron-diffraction studies by Plumier and his colleagues,² is realized in a tetragonally distorted garnet with octahedral ions Mn^{3+} — $\text{Ca}_3\text{Mn}_2\text{Ge}_3\text{O}_{12}$ (MnGeG) below the Néel temperature (13.85 K). This structure can be represented in a simplified manner as two two-dimensional crosses, in which the magnetic moments lie in two mutually perpendicular planes (110) and form an angle $\theta_0 = 39^\circ$ with the tetragonal axis [001] (the Z axis).

Investigations of the magnetic properties of the single crystal MnGeG show^{3,4} that an external magnetic field induces in this garnet a metamagnetic phase transition (PT), which cannot be described either by a model of the two-sublattice metamagnet or with the help of the mechanism of superexchange ordering of orbitals, proposed by Kugel' and Khomskii.⁵

In this work, we attempted to study in detail the PT indicated in MnGeG by the method of magnetostriction, which, in studying different spin-reorientation transitions, is generally more informative than magnetization methods.

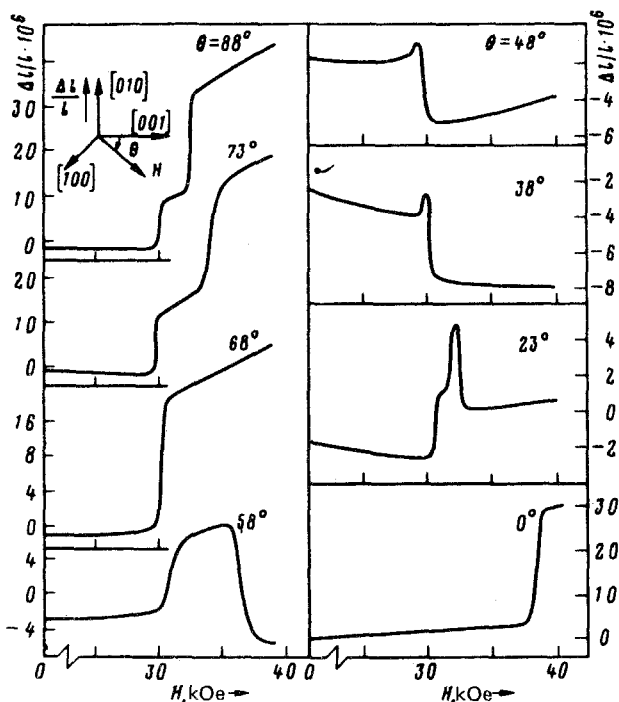


FIG. 1. Magnetostriction isotherms of MnGeG at 4.2 K for a field oriented in the (010) plane.

The magnetostriction ($\Delta l/l$) was measured by a capacitance transducer⁶ consisting of $2 \times 2 \times 2$ -mm MnGeG single crystals with predominant orientation of Jahn-Teller domains. The results of the measurements were rescaled to a single-domain specimen.³ The crystals were oriented by the x-ray method to within 0.5° . A special frequency-voltage converter permitted recording on an XY plotter the field dependence of the signal, which is proportional to the change in the frequency of the generator, in whose generating circuit the capacitance transducer was connected. In order to produce a transverse magnetic field, we used a superconducting magnet, constructed in the form of Helmholtz coils.

Figure 1 shows a number of characteristic isotherms of magnetostriction in the (010) plane. We shall point out their most significant features. Near [100] ($\theta = 88$ and 73°) $\Delta l/l$ attains a maximum value (40×10^{-6}) and has two positive jumps. The magnitude of the critical field H_c of the low-field jump 1 does not depend on θ near [100], while the field of the high-field jump 2 increases with increasing θ . For $\theta = 68^\circ$, only jump 1 is observed, while with further increase in θ two jumps again arise and, in addition, jump 2 becomes negative. At $\theta = 48, 38$ and 23° the difference in the values of H_c of both jumps is only ~ 0.8 kOe. A single positive jump is observed along the tetragonal axis [001].

In the (001) plane, for all field orientations, the magnetostriction isotherms exhibit a single jump ($\sim 15 \times 10^{-6}$), whose magnitude is nearly independent of the orientation

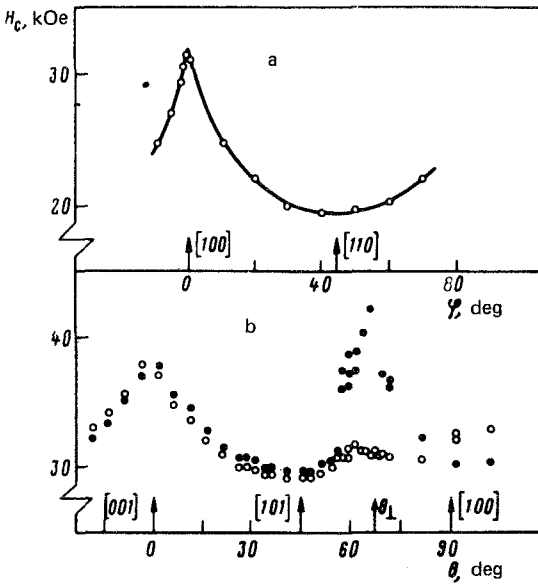


FIG. 2. Phase diagrams of MnGeG at 4.2 K for fields oriented in the (a) (001) and (b) (010) planes. Different points correspond to phase transitions in different pairs of antiferromagnetic sublattices.

of H . The values of the fields H_c , corresponding to jumps in magnetostriction, decrease as the [110] axis is approached.

The phase transition diagrams constructed from the measurements of $(\Delta l/l)(H)$ for the crystal MnGeG (Fig. 2) can be explained on the basis of the model of an anisotropic metamagnet⁷ with four local anisotropy axes, which corresponds experimentally to the observed magnetic structure of MnGeG.² The projection of this structure on the (010) plane is shown in Fig. 3(a).

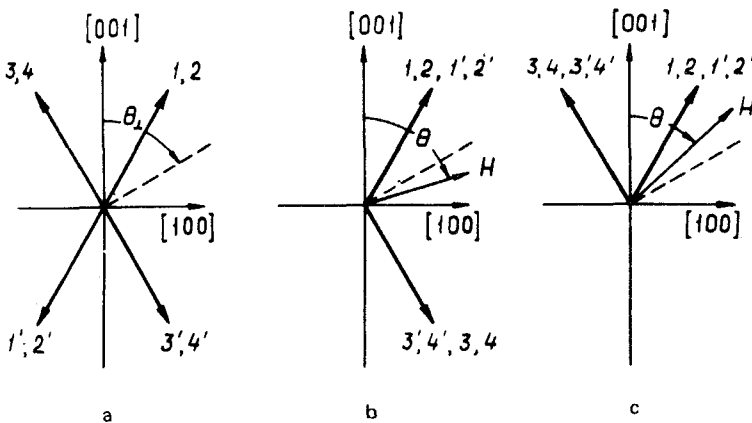


FIG. 3. Projection of the magnetic structure of MnGeG on the (010) plane for $H = 0$ (a); $H > H_c, \theta > \theta_1$ (b) $H > H_c, \theta < \theta_1$ (c).

In weak fields, magnetic moments of all sublattices tilt away from the local axes toward the direction of the field. As H is increased, a pairwise "collapse" of the antiferromagnetic sublattices, associated with a single local axis, occurs. For unsymmetrical orientations of H , in general, there should be four phase transitions.

Since (010) is a symmetry plane of the magnetic structure of MnGeG, for it there are two phase transition curves, which corresponds to the phase diagram in Fig. 2(b). In this plane, there is some distinguished field orientation (θ_1)—the direction perpendicular to the projection of the local axis on the (010) plane—near which only a single phase transition is observed experimentally. As is evident from Fig. 3, the passage through θ_1 in a strong magnetic field is accompanied by a change in the spin configuration of MnGeG. This is manifested on the magnetostriction isotherms as a change in the sign of the second jump (see Fig. 1, $\theta > 68^\circ$ and $\theta < 68^\circ$).

The phase diagram of MnGeG can be explained on the basis of the thermodynamic potential, which, in a system of coordinates fixed to the axes of the crystal, has the form

$$\Phi = \sum_{i=1}^4 \left\{ J_1 \mathbf{M}_i \mathbf{M}'_i + J'_1 \sum_{j \neq i} \mathbf{M}_i \mathbf{M}'_j + J_2 \sum_{j > i} \mathbf{M}_i \mathbf{M}_j + \mathbf{M}'_i \mathbf{M}'_j \right\} + \sum_{\alpha} \left[\frac{1}{2} K_1 (M_{iz}^{(\alpha)} \cos \theta_0 + M_{ix}^{(\alpha)} \sin \theta_0 \cos \varphi_{0i} + M_{iy}^{(\alpha)} \sin \theta_0 \sin \varphi_{0i})^2 - H M_i^{(\alpha)} \right]. \quad (1)$$

Here J_1, J'_1 and J_2 are the exchange-interaction parameters for the first and second nearest neighbors ($J_1, J'_1, J_2 > 0$); K_1 is the anisotropy constant ($K_1 < 0$); θ_0 and φ_{0i} are the polar and azimuthal angles of the i th local axis; \mathbf{M}_i and \mathbf{M}'_i are the magnetic moments of the pairs of antiferromagnetic sublattices that belong to the i th local axis; and the index α indicates summation with respect to the sublattices.

We note that the computed phase diagram agrees with experiment if $J_1, J'_1, J_2 \sim \frac{1}{10} |K_1|$. If the angle θ_1 is known and if the fact that the local axis does not lie in the (010) plane is taken into account, we can easily determine the angle θ_0 . According to our data, it is 33° in MnGeG.

The different magnitudes of the deformations of the crystal after the second phase transition for $\theta > \theta_1$ and $\theta < \theta_1$ can be qualitatively explained by examining the transitions from the initial equilibrium state at $H = 0$ (Fig. 3a) into the two spin configurations, shown in Figs. 3b and 3c, respectively. Writing the magnetoelastic energy of the tetragonal system with the eight sublattices as one-half the sum \mathbf{m}_i and one-half the difference \mathbf{l}_i of the magnetic moments associated with the i th local axis, we find that the different resulting deformations U_{yy} after the second phase transition are due to terms of the form $B_{\alpha} \Delta \sum_{ij} m_{i\alpha} m_{j\alpha} = B_{\alpha} \Delta M_{\alpha}^2$ ($\alpha = x, z$). Here B_x and B_z , in general, are different magnetoelastic constants, and M_{α} is the corresponding component of the resulting magnetization. Here the terms with \mathbf{l}_i , which give identical contributions to the deformation for $\theta > \theta_1$ and $\theta < \theta_1$ (terms with m_{iy} do not experience jumps), are not included.

It is evident from Fig. 3 that spin configurations with $\theta \geq \theta_1$ have different components of the resulting magnetization. Thus, by assuming that $B_x > 0$ and B_z is small,

we find that $U_{yy} > 0$ for $\theta > \theta_1$ and $U_{yy} \simeq 0$ for $\theta < \theta_1$, in agreement with experiment, i.e., the resulting magnetostrictional deformation vanishes; this effect is manifested in the experimental curves $(\Delta l/l)(H)$ as a jump with opposite sign.

A numerical calculation and comparison with experiment will be presented in greater detail in a separate paper.

We thank A. S. Borovik-Romanov and R. Z. Levitin for a useful discussion of the results.

¹Z. A. Kazei, P. Novak, and V. I. Sokolov, Zh. Eksp. Teor. Fiz. **83**, 1483 (1982) [Sov. Phys. JETP, **56**, 854, 1982].

²R. Plumier and D. Esteve, Solid State Commun. **31**, 921 (1979).

³Z. A. Kazei, B. V. Mill', and V. I. Sokolov, Pis'ma Zh. Eksp. Teor. Fiz. **31**, 338 (1980) [JETP Lett. **31**, 308 (1980)].

⁴D. Esteve, R. Plumier, P. Feldman, and H. LeGall, Phys. Status Solidi A **57**, K83 (1980).

⁵K. I. Kugel' and D. I. Khomskii, Pis'ma Zh. Eksp. Teor. Fiz. **23**, 264 (1976) [JETP Lett. **23**, 237 (1976)].

⁶Z. A. Kazei, M. V. Levanidov, and V. I. Sokolov, Prib. Tekh. Eksp., No. 1, 196 (1982) [Instrum. Exp. Tech. (USSR) **25**, 223 (1982)].

⁷A. P. Mitsek, N. P. Kolmakova, and D. I. Sirota, Phys. Status Solidi A **65**, 503 (1981).

Translated by M. E. Alferieff

Edited by S. J. Amoretty